P-ISSN 2586-9000
E-ISSN 2586-9027
Homepage : https://tci-thaijo.org/index.php/SciTechAsia
Science & Technology Asia
Vol.28 No.2 April - June 2023
Page: [125-142]
Original research article

Slope Stability of Riverbank during Flood in Bengkulu City, Indonesia (A case study of Nakau Segment)

Lindung Zalbuin Mase[1,*], Reki Sunanda[1], Fazriaty Utami[1], Mira Sintia Wahyuni[1], Muhammad Disa Syafrizal[1], Mutiara Azzahra Putri[1], Suraparb Keawsawasvong[2]

[1]*Department of Civil Engineering, Faculty of Engineering, University of Bengkulu, Bengkulu 38371, Indonesia*
[2]*Department of Civil Engineering, Thammasat School of Engineering, Thammasat University, Pathum Thani 12120, Thailand*

Received 12 April 2022; Received in revised form 18 September 2022
Accepted 28 September 2022; Available online 14 June 2023

ABSTRACT

The Nakau Segment area serves as the connecting zone between Bengkulu City and Central Bengkulu Regency. Socio-economic development has been significant within the last 20 years. Several housing zones are located near the riverbank of the main river called the Muara Bangkahulu River. The riverbank could undergo slope failure during floods. It is important to study slope stability in this area. This study is initiated by collecting undisturbed soil samples in the study area and measuring slope geometry. Furthermore, laboratory tests to check the soil's physical-engineering properties are conducted. Those properties and geometries are used as input parameters in finite element simulation. Several results including failure mechanism, total displacement, and factor of safety are presented in micro-zonation maps. The results show that the factor of safety of the river bank is generally observed to vary from 1.5 to 2.0, especially in the eastern and western parts of the river. The results indicate the failure tendency could occur in the slope body which is consistent with slope failure observed in the field. The results of this study could be used as a consideration to design slope countermeasure efforts in the study area.

Keywords: Finite element method; Muara Bangkahulu River; Nakau segment; Slope failure

1. Introduction

Misliniyati et al. [1] mentioned that Bengkulu City has been known as one of the earthquake-prone areas in Indonesia. Nevertheless, the city is also very vulnerable to climate change impact as reported by Mase et al. [2]. In April 2019, a huge flood that is called the2019 Bengkulu

***Corresponding author:** lmase@unib.ac.id

Flash Flood hit Bengkulu City. Areas located along the Muara Bangkahulu River, the main river in the Central Part of Bengkulu Province, were inundated for days and many people were evacuated to temporary camps. In addition, massive slope failures were found after the flood.

Bengkulu City is one of the areas that underwent flood impacts in 2019. This city is a part of the downstream Muara Bangkahulu sub-watershed. A district that significantly experienced the flood impact is Sungai Serut District. Several segments recorded as the most impacted areas during the flood in this district are Muaro Kualo Segment [3], Tanjung Agung Segment [4], Semarang-Surabaya Segment [5, 6], and Nakau Segment. Studies conducted by several local researchers [3-6] reported that of all segments, Nakau Segment is directly bordered by the Central Bengkulu Regency where the spring of Muara Bangkahulu River exists. So far, a study related to slope stability during floods in Nakau Segment has not been performed. Therefore, it is important to perform a study of slope stability during the flood in the study area.

There are several methods to estimate slope stability. They are the limit equilibrium method [7], the finite element method [3], and the finite difference method [8]. Among these methods, the finite element method is known as the most familiar method for predicting slope stability. This method tends to be more selected because the calculation process is fast and the result is generally consistent with field conditions. In addition, the use of the finite element method could result in the factor of safety (FS) and total displacement. Several researchers such as, Chheng and Likitlersuang [9], Ukritchon and Keawsawasvong [10], Mase et al. [11], and Huyn et al. [12] have confirmed that the use of the finite element method is generally appropriate to solve the stability problem for several cases, such as deep excavation, bearing capacity, and liquefaction during an earthquake. For slope stability analysis at the riverbank area, Mase et al. [3] also stated that the use of the finite element model is appropriate to observe the failure mechanism on riverbank slopes. It can be concluded that the use of the finite element method is recommended to solve stability problems in geotechnical engineering, especially for sloping ground.

The sloping ground of the riverbank is very critical to failure during a flood. Udomchai et al. [13], Thi and Minh [14], and Liang et al. [15] mentioned that slope failure during floods is generally initiated by massive erosion at the slope toe and slope body. The pattern yielded by erosion could be the path for water to infiltrate into soil mass. Once the process of soil saturation happens, the soil shear strength could decrease. On another side, due to the saturated condition, soil mass becomes heavier. At this condition, a heavier soil mass and a decrease in soil shear strength could influence the movement of soil mass at the sloping ground [3]. Therefore, it is important to know the slope stability under saturated conditions during floods.

This paper presents a finite element analysis to analyze slope stability along Nakau Segment. The initial step is begun by conducting a site investigation at Nakau Segment. Furthermore, the laboratory test is conducted to obtain physical and engineering properties. The finite element simulation is conducted to determine the FS of slope and maximum displacement in the study area. The map of slope vulnerability is composed to interpret safe and unsafe zones. In general, this study could provide information related to the slope failure potential in the study area. The results are also able to be used by the local government of Bengkulu City as the consideration for slope countermeasure efforts in the study area.

2. Study Area

Fig. 1 shows the study area layout. Nakau Segment is located in the eastern part

of the Muara Bangkahulu River. According to River Territory Office (RTO) [16], Nakau Segment is the first segment in the Sub-watershed of Downstream Muara Bangkahulu, in Bengkulu City. Nakau Segment is bordered by Surabaya Segment in the western part and Central Bengkulu Regency in the eastern part. Since Nakau Segment is bordered by the neighboring regency, the development of this segment as the socio-economic center is gradually growing. In this area schools, tourist areas, and housing areas exist. This area is also the entrance to Bengkulu City from Central Bengkulu Regency. This area is very important to support the economic aspects of Bengkulu City. In short, economic and social activities are very dense here.

In Fig. 1, there are 20 cross-sections, namely CS-1 to C-20, that are observed in this study. Those cross-sections are located on the riverbank of the Nakau Segment. The riverbank slope height in the study area is varied from 1 to 7 m and the width is varied from 1 to 6 m. The slope inclination for those observed slopes varied from 18° to 72° (Fig. 2).

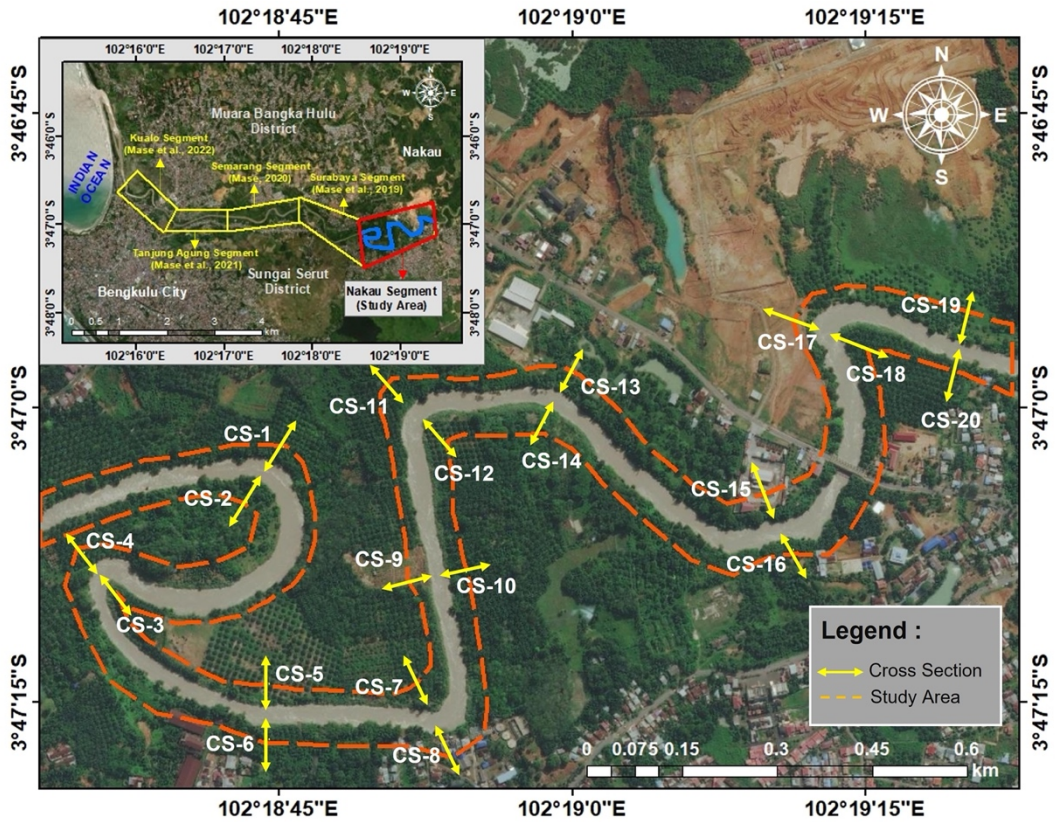

Fig. 1. Location of the study area.

In the study area, undisturbed soil sampling is conducted on riverbank slopes. Undisturbed samples are then tested in the laboratory to collect physical properties and soil engineering properties. Physical properties, such as water content, unit weight, and specific gravity are addressed to obtain soil characteristics. Engineering properties are addressed to obtain shear strength parameters, such as cohesion and internal friction angle. There are 20 spots of undisturbed samples spreading along the riverbank slopes. After laboratory tests, both physical and engineering properties are used as the input parameters for slope stability analysis.

The summary of soil properties in the Nakau Segment can be seen in Table 1. It can be observed that the soil type in the study area is categorized as sandy soil. Based on the Unified Soil Classification System or USCS, those sandy soils are classified as poorly graded sand (SP), well-graded sand (SW), silty sand (SM), and clayey sand (SM). Also, a minor silty soil is classified as low plasticity silt (ML). The soil type in each cross-section can be categorized as homogenous soil.

Based on physical properties, the water content of sandy soils (w) varies from 18 to 73%, whereas silty soil is about 22%. The densities of soils under bulk (γ_b), dry (γ_d), and saturated (γ_{sat}) conditions show that the range of densities varies from 11 to 19 kN/m^3. It is predicted that the coefficient permeability for sandy soils in the study area varies from 0.8 to 1 m/day [17, 18]. In addition, based on the recommendation suggested by Carter and Bentley [17] and Bowles [18], Young's modulus (E_{ref}) varies from 1×10^5 kN/m^2 to 5×10^5 kN/m^2 with Poisson's ratio of about 0.25 to 0.42. The grain size analysis showed that the coefficient of uniformity (C_u) is observed to vary from 1.67 to 2.82 and the coefficient of curvature (C_c) is observed to vary from 0.82 to 1.25. For soil containing fines content, the Atterberg limits test shows that liquid limit (LL) is observed to vary from 40 to 45%, plastic limit (PL) is observed to vary from 31 to 42%, and shrinkage limit (SL) is observed to vary from 21 to 22%. The plasticity index (PI) is observed to vary from 3 to 9%.

For engineering properties, two main tests are conducted, i.e., the direct shear test and the unconfined compression test. A direct shear test is conducted to determine the shear strength of cohesionless soil, whereas the unconfined compression test is addressed for cohesive soils. Based on experiments, soil cohesion (c) for sandy soils in the study area is observed to vary from 1.33 to 3.63 kN/m^2 whereas internal friction angle (ϕ) is observed to vary from 28.63° to 41.99°. For the unconfined compression test, it is known that undrained shear strength (s_u) is about 40.166 kN/m^2. Those parameters listed in Table 1 are used as the input parameters for slope stability analysis.

3. Theory and Method

3.1 Finite element analysis of slope stability

The level of slope stability is defined by a factor that represents the comparison between resisting force and driving force. This factor is known as FS. Stark and Ruffling [19] mentioned that for a slope located in an area with a high-environmental effect, an FS of 1.5 could be implemented. Since this study area is located in an area where natural activity such as floods frequently occurred, the use of FS of 1.5 can be considered.

The use finite element method is selected and common in geotechnical engineering. Matsui and San [20], Dawson et al. [21], and Zhang et al. [22] mentioned that the use of finite elements to solve slope stability problems is accurate and relatively consistent with field observation. Those researchers also suggested that the use of the Mohr-Coulomb model for soil materials could be implemented in the analysis of

finite elements. In finite element simulation, the procedure to analyze slope stability is defined into a calculation method called the reduction of shear strength. This calculation method emphasizes the evaluation of slope stability by gradual reduction of shear stress. Therefore, during the iteration process, the incremental condition is considered in the calculation.

Table 1. Summary of soil properties in the Nakau Segment.

Soil Parameters	Unit	Cross-Sections									
		CS-1	**CS-2**	**CS-3**	**CS-4**	**CS-5**	**CS-6**	**CS-7**	**CS-8**	**CS-9**	**CS-10**
Physical properties											
Water content (w)	%	18.82	22.96	26.76	21.84	56.28	23.07	30.11	54.04	45.26	72.79
Specific gravity (G_s)	-	2.67	2.65	2.66	2.81	2.67	2.66	2.66	2.66	2.65	2.67
Bulk density (γ_b)	kN/m^3	16.83	14.36	17.38	17.78	19.58	14.21	17.25	18.89	18.57	18.06
Dry Isi (γ_d)	kN/m^3	14.16	11.68	13.72	14.92	12.56	11.54	13.26	12.26	12.79	10.45
Saturated density (γ_{sat})	kN/m^3	20.70	19.88	19.32	20.83	16.36	19.88	18.86	16.49	17.16	15.37
Void ratio (e)	-	0.50	0.61	0.71	0.61	1.50	0.61	0.80	1.44	1.20	1.94
Coeff of permeability (k)	m/day	0.81	0.85	0.89	1.E-04	0.83	0.86	0.91	0.67	0.92	1.02
Soil Elasticity											
Young modulus (E_{ref})	kN/m^2	1.E+05	1.E+05	1.E+05	1.E+05	1.E+05	1.E+05	1.E+05	2.E+05	1.E+05	5.E+05
Poisson's ratio (v)	-	0.25	0.25	0.26	0.42	0.25	0.26	0.26	0.33	0.25	0.36
Grain size analysis											
No.200 passing	%	0.10	2.15	0.85	50.81	0.45	3.80	0.50	6.35	0.00	1.45
No.200 retaining	%	99.90	97.85	99.15	49.19	99.55	96.20	99.50	93.65	100.00	98.55
Coeff of uniformity (C_u)	-	1.67	1.68	1.69	-	1.71	1.80	2.10	3.22	2.10	2.66
Coeff of curvature (C_c)	-	0.82	0.84	0.87	-	0.85	1.25	1.07	0.86	1.08	0.97
Atterberg limits											
Liquid limit (LL)	%	-	-	-	45.327	-	-	-	40.336	-	-
Plastic limit (PL)	%	-	-	-	42.056	-	-	-	32.964	-	-
Plasticity index (PI)	%	-	-	-	3.272	-	-	-	7.372	-	-
Shrinkage limit (SL)	%	-	-	-	-	-	-	-	-	-	-
Direct Shear Test											
Soil cohesion (c)	kN/m^2	1.94	2.59	1.94	-	3.23	1.33	2.79	3.63	2.73	2.58
Internal friction angle (ϕ)	^{o}	41.99	39.05	38.36	-	37.65	37.98	29.95	30.18	31.03	30.85
Unconfined compression test											
Compression (q_u)	kN/m^2	-	-	-	80.333	-	-	-	-	-	-
Shear strength (s_u)	kN/m^2	-	-	-	40.166	-	-	-	-	-	-
Soil Classification	USCS	SP	SP	SP	ML	SP	SP	SP	SC	SP	SW

Soil Parameters	Unit	Cross-Sections									
		CS-11	**CS-12**	**CS-13**	**CS-14**	**CS-15**	**CS-16**	**CS-17**	**CS-18**	**CS-19**	**CS-20**
Physical properties											
Water content (w)	%	39.47	30.44	40.26	55.64	41.23	69.61	46.13	46.06	43.54	35.85
Specific gravity (G_s)	-	2.67	2.65	2.66	2.67	2.66	2.65	2.68	2.66	2.65	2.67
Bulk density (γ_b)	kN/m^3	18.42	16.10	16.10	24.28	17.45	18.28	19.96	17.33	17.09	17.17
Dry Isi (γ_d)	kN/m^3	13.21	12.34	11.48	15.60	12.36	10.78	13.66	11.87	11.92	12.65
Saturated density (γ_{sat})	kN/m^3	17.80	18.79	17.67	16.39	17.56	15.50	17.19	17.13	17.33	18.19
Void ratio (e)	-	1.06	0.81	1.07	1.48	1.09	1.84	1.24	1.23	1.15	0.96
Coeff of permeability (k)	m/day	0.82	1.08	0.89	0.86	0.88	0.77	0.76	0.78	0.67	0.83
Soil Elasticity											
Young modulus (E_{ref})	kN/m^2	1.E+05	5.E+05	1.E+05	1.E+05	1.E+05	2.E+05	2.E+05	2.E+05	2.E+05	1.E+05
Poisson's ratio (v)	-	0.25	0.36	0.26	0.26	0.25	0.26	0.26	0.26	0.25	0.24
Grain size											
No.200 passing	%	5.10	4.95	2.55	4.00	2.65	6.10	6.65	3.95	2.40	0.05
No.200 retaining	%	94.90	95.05	97.45	96.00	97.35	93.90	93.35	96.05	97.60	99.95
Coeff of Uniformity (C_u)	-	1.87	2.82	1.66	2.07	1.68	2.14	1.68	2.12	2.10	1.71
Coeff of Curvature (C_c)	-	0.92	0.99	0.72	0.92	0.83	1.03	0.85	1.05	1.04	0.87
Atterberg limits											
Liquid limit (LL)	%	-	-	-	-	-	40.926	-	-	41.029	-
Plastic limit (PL)	%	-	-	-	-	-	31.942	-	-	32.529	-
Plasticity index (PI)	%	-	-	-	-	-	8.984	-	-	8.500	-
Shrinkage limit (SL)	%	-	-	-	-	-	21.732	-	-	22.606	-
Direct shear test											
Soil cohesion (c)	kN/m^2	2.91	2.19	2.62	2.25	2.95	3.70	2.24	3.62	3.52	2.61
Internal friction angle (ϕ)	^{o}	29.75	28.95	29.51	30.59	30.70	28.85	29.99	28.63	28.94	30.51
Unconfined compression test											
Compression (q_u)	kN/m^2	-	-	-	-	-	-	-	-	-	-
Shear strength (s_u)	kN/m^2	-	-	-	-	-	-	-	-	-	-
Soil Classification	USCS	SP	SW	SP	SP	SP	SC	SP	SM	SC	SP

Dyson and Tolooiyan [23] mentioned that the shear strength reduction method is applicable to precisely estimate each optimized reduction stage during finite element simulation. The implementation of shear strength reduction is also reliable for slope stability cases, such as heterogeneous slope [24], reinforced slope [25], and rock slope [26]. It is, therefore, appropriate to use the shear strength reduction method to analyze the slope stability of the Nakau Segment.

In finite element simulation, several input parameters for checking slope stability are required. The input parameters are generally determined based on laboratory and field tests conducted on soil samples. The main input parameters are related to physical properties including soil type, soil density or unit weight (γ), modulus of elasticity (E_{reff}), and Poisson's ratio (ν). For engineering properties, several parameters including shear strength parameters (soil cohesion or *c*, internal friction angle (ϕ), dilatancy angle (ψ), and permeability coefficient (*k*) are used as the input parameters. During the analysis, there are two steps of calculation considered in the analysis. Since this study presents the natural slope, the initial phase of analysis is to load the model with gravity loadings or overburden pressure. The next step is conducted by the calculation analysis using the shear strength reduction method. The output based on the finite element is a factor of safety (FS). The virtual results called deformed mesh and total displacement are also presented.

3.2 Research framework

This study emphasizes the implementation of the finite element to check the slope stability of the riverbank slope in the Nakau Segment, Bengkulu City, Indonesia. This study is first conducted by collecting important data, such as the geometry of the slope in the Nakau Segment, and the average height of river water level during the flood. Based on RTO [16], the average height of river water level during floods within the last 20 years is about 4 to 6 m above the river bed. The illustration of the condition of the slope and river water during the flood is presented in Fig. 2. In Fig. 2, it can be observed that the position of the river water level during the critical condition has inundated the riverbank slope. Under this condition, the slope can be fully saturated during the flood.

Afterward, the next step is laboratory testing. During the field observation, the undisturbed sampling is collected and tested in the laboratory. There are two kinds of tests conducted in this study, i.e., the physical properties test and the engineering properties test. The laboratory tests are addressed to determine soil classification, soil characteristics, and parameters for finite element simulation. The data obtained from field observation and laboratory tests are used as input materials for finite element simulation. Input materials for finite element simulation include the unit weight of soil, shear strength, modulus elasticity, Poisson's ratio, permeability coefficient, and so on as listed in Table 1.

During the simulation, there are two construction stages. The first stage is to load gravity loadings of the slope model. This procedure is recommended when the soil surface, the layering, or the phreatic level is non-horizontal. Gravity loading always produces an equilibrium stress state. During the gravity loading application, both soil weight and pore pressures are activated. The second stage is to analyze the slope stability. A calculation procedure, namely the reduction of shear strength, is implemented to obtain FS. To depict the zonation of the slope during the flood, the micro-zonation maps including the FS map and total displacement map are composed. The maps are composed using the Kriging and Gridding Interpolation method [27].

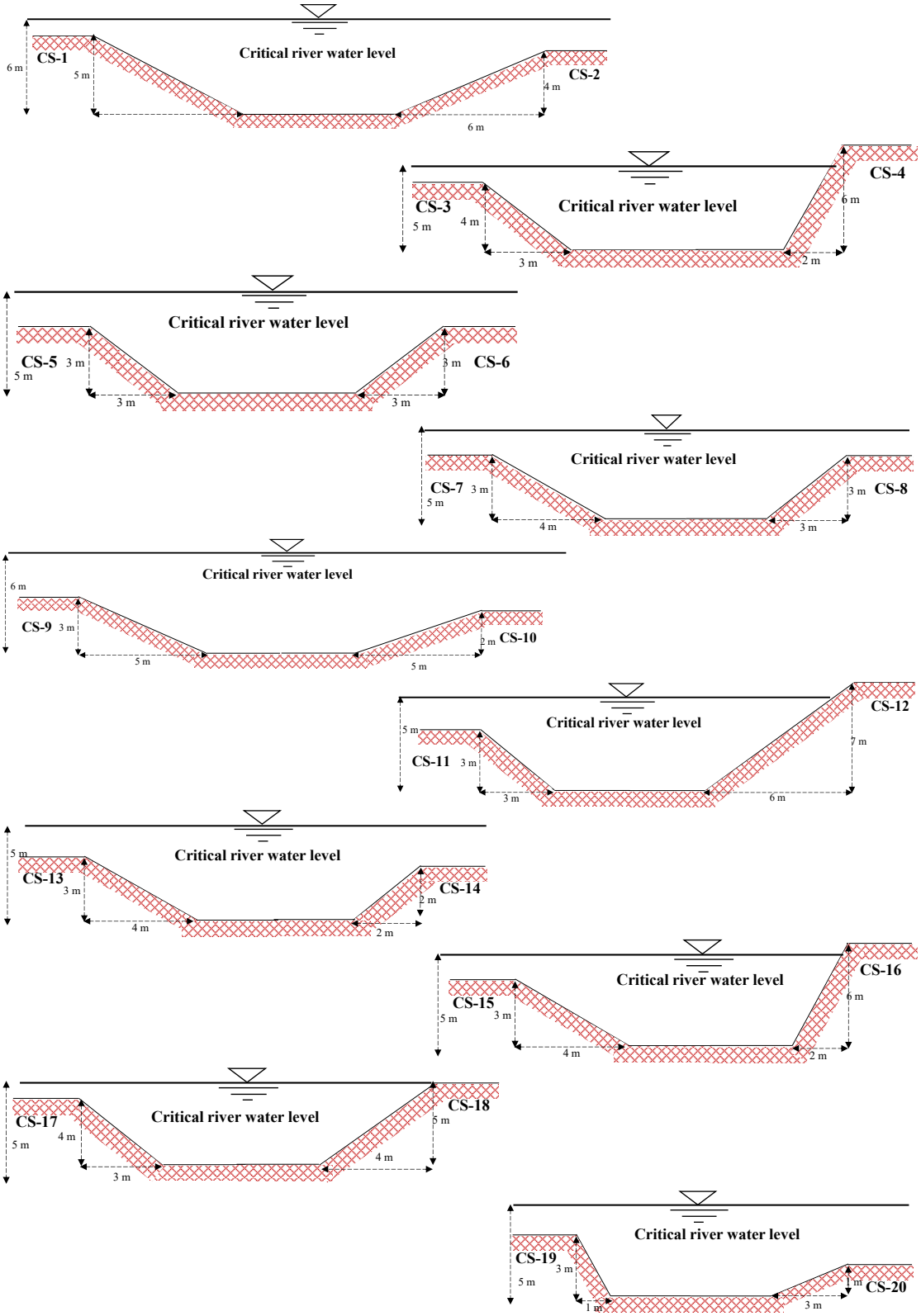

Fig. 2. Illustration of the height of river water level and slope condition during flood [16].

4. Results and Discussion

4.1 Slope stability analysis

Figs. 3 and 4 present the results of finite element simulation for the slope along the Nakau Segment during the flood. In this study, there are 7 cross-sections selected as represented slopes. They are CS-1, CS-4, CS-7, CS-12, CS-13, CS-16, and CS-17. Those cross-sections are located at the river meander. In this zone, erosion and sedimentation are massively found. This is because the river stream during floods eroded and dumped the riverbank. Sedimentation and erosion are generally found in the meander zone of the river.

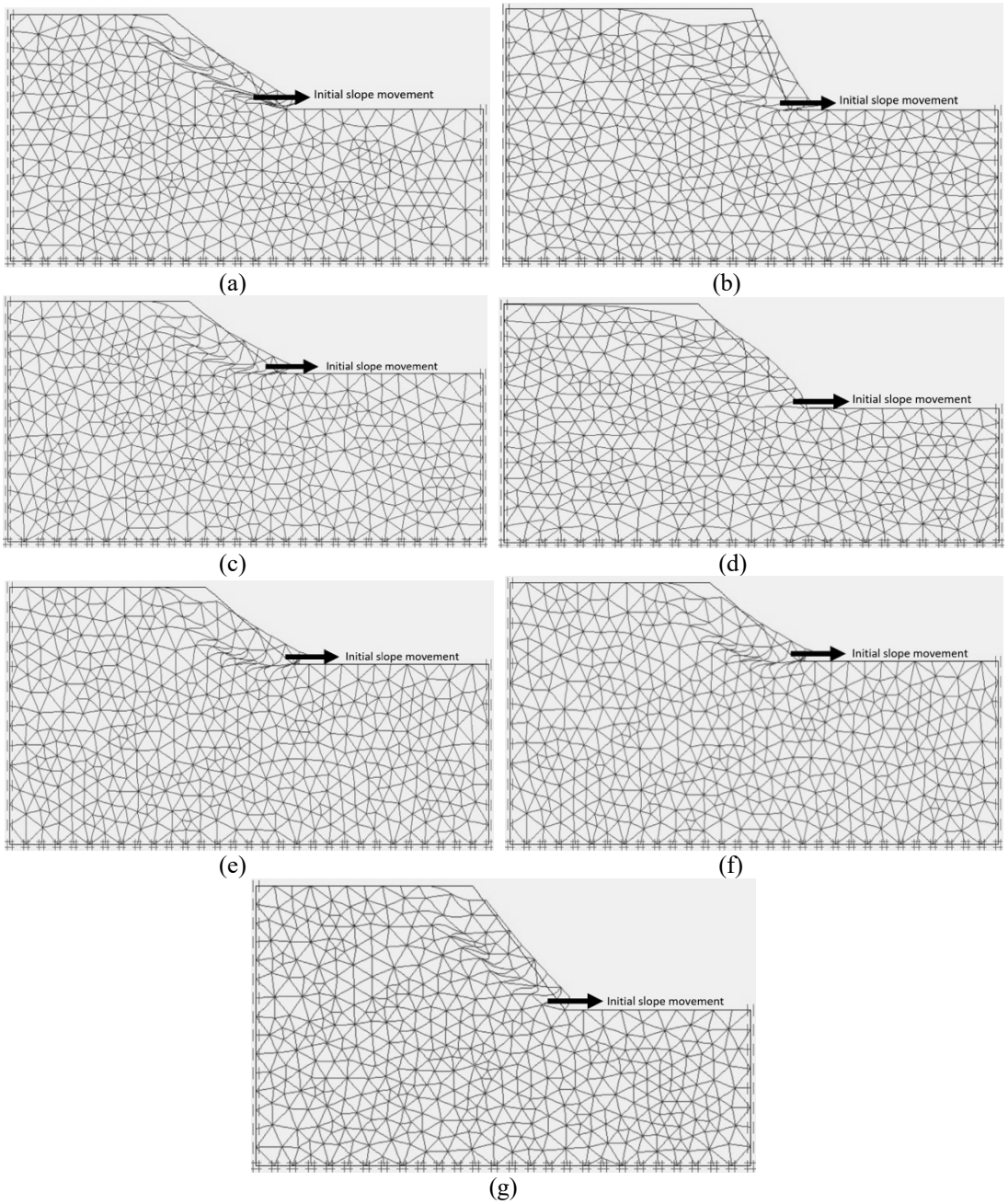

Fig. 3. Slope deformation (a) CS-1, (b) CS-4, (c) CS-7, (d) CS-12, (e) CS-13, (f) CS-16, (g) CS-17.

Fig. 3 presents the slope deformation tendency during the flood. In Fig. 3, it can be observed that meshes on the slope model tend to undergo deformation horizontally. There is an increase in the water level. The increase of river water level is then followed by the infiltration into slope mass. The increase in river water level could increase the effective stress. Under this condition, there is a reduction of shear strength. In line with this, the soil mass becomes heavier. Since it is located on sloping ground, the driving force tends to be larger. Fig. 3 also shows that the movement of the slope is generally started at the slope toe.

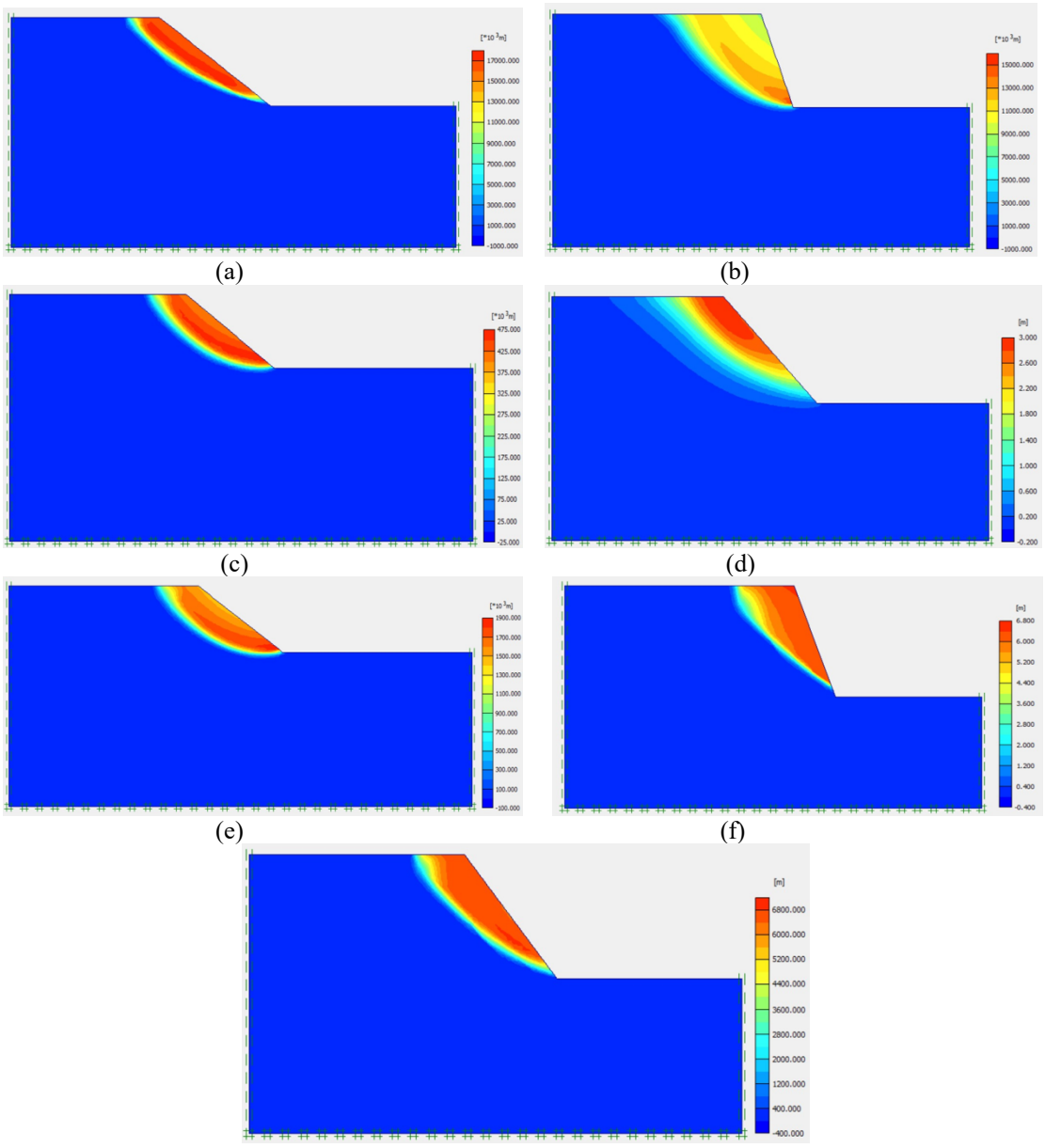

Fig. 4. Failure Mechanism (a) CS-1, (b) CS-4, (c) CS-7, (d) CS-12, (e) CS-13, (f) CS-16, (g) CS-17.

Fig. 4 presents the failure mechanism from finite element simulation for seven represented slopes. In Fig. 4, it can be observed that the type of slip surface resulting from the simulation is generally a circular slip surface. The surface tendency could be also shaped as a wedge plain as shown in Fig. 4f. The wedge plain on the slip surface indicates that the soil mass movement could behave as a lump of soil mass once slope failure happens. Based on the results, slope movement is generally initiated at the slope toe. Table 2 presents the summary of FS and total displacement from finite element simulation for all studied cross-sections. In Table 2, the analysis using the finite element method also shows that the total displacement of the slope is observed to vary from 1.304 m to 8.641 m. FS in the study area is predicted to vary from 1.002 to 1.781. It indicates that there are unsafe and safe slopes during the flood.

Table 2. Summary of FS and total displacement.

Cross-sections of slopes	The Factor of Safety (FS)	Total Displacement (m)
C-1	1.226	1.331
C-2	0.876	1.610
C-3	1.124	8.641
C-4	1.464	1.933
C-5	1.002	2.442
C-6	0.837	3.628
C-7	1.630	3.632
C-8	1.003	1.670
C-9	1.781	4.028
C-10	1.003	1.559
C-11	0.774	2.845
C-12	0.919	1.750
C-13	1.287	1.349
C-14	1.004	1.740
C-15	1.144	4.267
C-16	0.960	1.685
C-17	1.055	1.417
C-18	1.224	1.304
C-19	1.620	1.660
C-20	1.244	2.239

It can be observed that the increase in river water level could result in unstable slope conditions in the study area. Generally, the slope inclination in the study area is varied from 18° and 71°, which indicates that the slopes in the study area are generally gentle to steep. A large slope inclination tends to result in a larger gravity movement [28]. Hampton et al. [29] mentioned that once the infiltration of water into soil mass happens, there is a change of soil unit weight from bulk condition to saturated condition. The increase in unit weight could increase the soil mass weight. Since the soil mass is at the inclined plane, the driving force of the soil tends to be larger. The increase in water level could decrease the soil shear strength, especially soil cohesion. The slickenside of soil could be formed and the soil mass could fail. Also presented in Table 2, most of the cross sections tend to have FS less than 1.5 which indicates that the slope could potentially collapse during the flood.

4.2 Slope vulnerability maps

Fig. 5 presents the distribution of FS along the Nakau Segment during the flood. It can be observed that generally, the riverbank at Nakau Segment is very vulnerable to slope failure. This is because FS values are generally less than 1.5. The areas with FS less than 1.5 are indicated with red shading on the map. Several parts could be categorized as stable zone because FS is more than 1.5. These parts are indicated by yellow shading in Fig. 5. Based on field observation conducted by Mase [6] along the downstream area of the Muara Bangkahulu River in Bengkulu City, many riverbank failures were observed during the 2019 Bengkulu Flash Flood. Nakau as one segment in Muara Bangkahulu River in Bengkulu City also underwent slope failures and it is generally consistent with the results of finite element analysis.

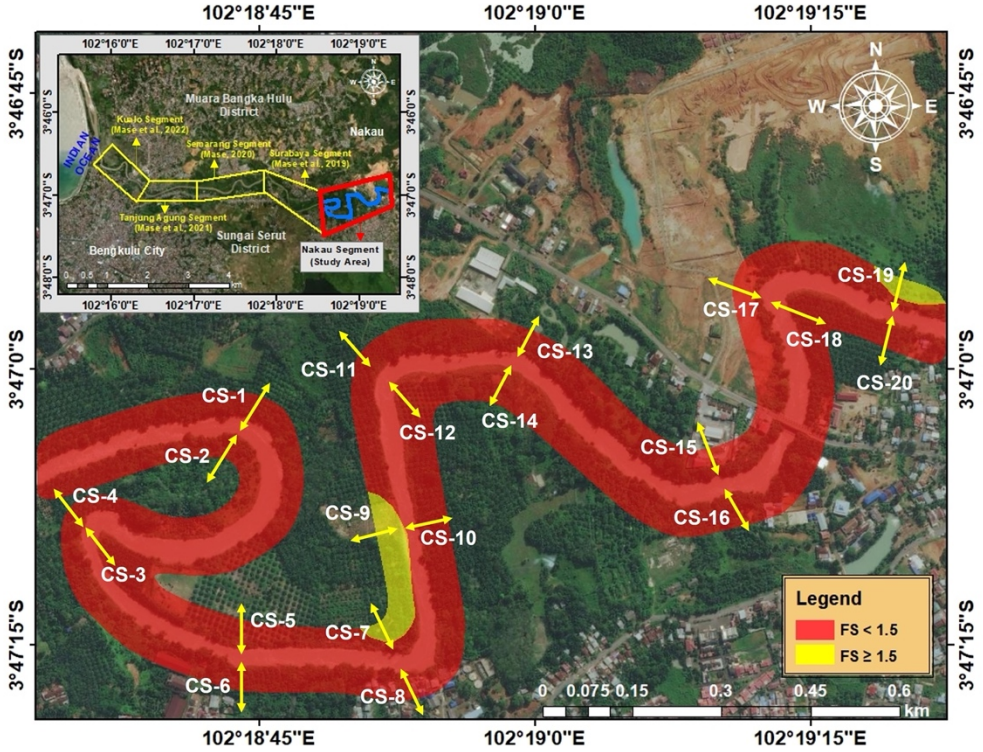

Fig. 5. FS map during the Bengkulu Flood in 2019 at Nakau Segment

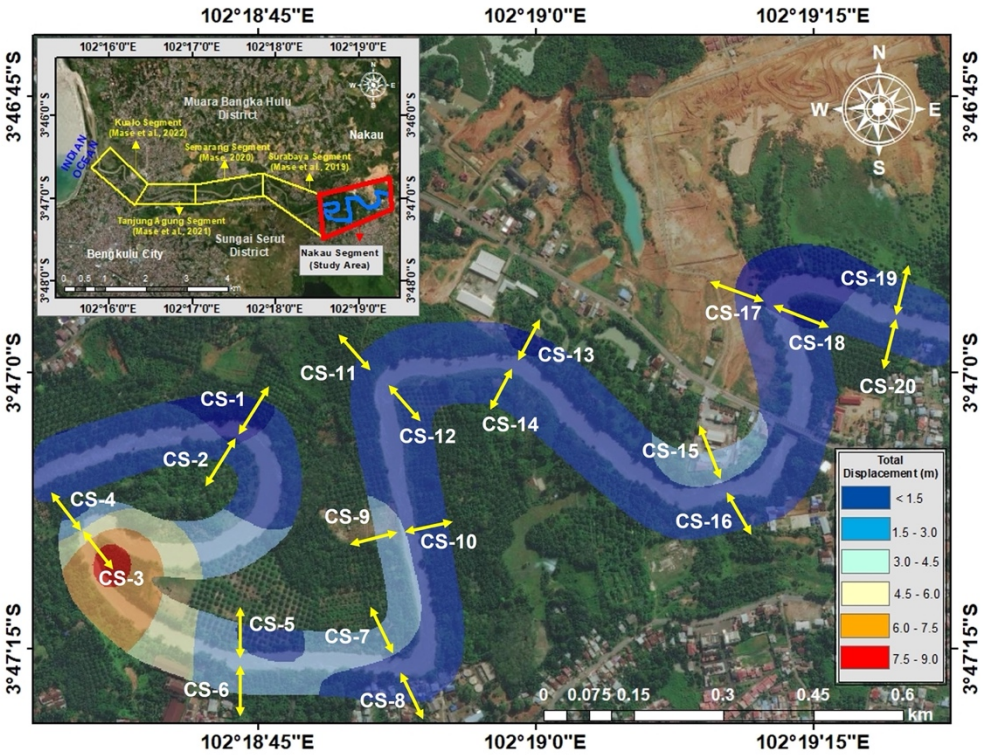

Fig. 6. Total displacement map due to flood at Nakau Segment.

Fig. 6 presents the distribution of total displacement of the riverbank slope at the Nakau Segment. As shown in Fig. 6, it can be observed that there are 6 zones of total displacement in the study area. The most dominant zone is where total displacement varied from 1.5 to 3.0 m. This zone is mostly found at many parts of the Nakau Segment. The value of total displacement varied from 3 to 4.5 m in the second dominant zone in Nakau Segment. This range generally heaps at the downstream area of the Nakau Segment in the western part. The highest total displacement of the slope is found also in the downstream area, especially at the meander parts of the Nakau Segment.

As presented in Figs. 5 and 6, it can be also observed that there are many meander lines in the Nakau Segment. Those meander lines are identified as the vulnerable zone to undergo slope failure. Meanders are one of the most distinctive features of fluvial environments [30, 31]. It should be noted that in the meander lines, both sedimentation and erosion could occur naturally [32]. The erosion could result in a scouring zone at the slope toe. The scouring zone at the same time also yielded a steeper slope due to the reduction of slope inclination as observed in several cross sections, such as CS-4, CS-16, and CS-19. At those cross sections, the inclination of the slope is relatively steep which indicates that there is a scouring effect changing slope inclination [33]. At those cross-sections, the potential mass movement due to the gravity effect could play important role in determining slope stability. Also, the type of failure for the steep slope is generally wedge failure as observed at CS-4 and CS-12 in Fig. 4. For the sedimented zone, the slope inclination tends to be gentler. This is because the sediment deposit was dammed at the slope toe. Under this condition, the slope should be more stable since there is a counterweight applied at the slope toe. Nevertheless, the effect could result in the narrowing of the river, as shown in several slopes, such as CS-9, CS-10, and CS-20. Since the river water tends to be inundated due to the existence of sediment materials, the process of infiltration could occur slowly and continuously at the riverbank slope toe [34]. Mizutani et al. [35] mentioned that, therefore, even though there is no flood, the process of infiltration occurs normally and could also reduce the soil shear strength and it is initially started also at the slope toe. The typical slope failure that generally occurs, is circular [36] as shown in CS-1, CS-7, and CS-13 in Fig. 4. In general, Osman and Thorne [37] and Thorne and Osman [38] mentioned that the combination between sedimentation and erosion in the river segment could contribute to the environmental effect. Therefore, the effort on river conservation, especially for river-watershed should be considered [39].

In line with Fig. 6, the maximum total displacement could significantly occur in CS-3 and CS-4. Those two slopes are positioned on the downstream meander at Nakau Segment. To reduce the potency of slope failure in the Nakau Segment, particularly in the meander zone, the slope countermeasure effort could be implemented, especially by anticipating the significant effect at the slope toe.

4.3 Prediction of FS

In this study, the mathematical model to estimate FS based on finite element simulation is conducted. Several parameters are assumed as contributing factors in determining FS. Those parameters are saturated unit weight (γ_{sat}), soil cohesion (c), and the ratio between friction angle (ϕ) and slope inclination (β). The parameters are correlated under multiple linear regression. The predicted FS at Nakau Segment can be estimated by using the following equation:

$$FS = 0.062\gamma_{sat} + 0.006c + 0.028\left(\frac{\tan\phi}{\tan\beta}\right). \quad (4.1)$$

In Eq. (4.1), FS is a factor of safety. R^2 for the proposed equation is 0.946. The observed data mean plots points between the results of finite element analysis and the prediction from Eq. (4.1) for each studied slope. It indicates the correlation that is proposed based on predicted FS (from Eq. (4.1)) and calculated FS (from finite element analysis) values are in good agreement with each other. To observe the performance of the model, the comparison between predicted FS and calculated FS is shown in Fig. 7. In Fig. 7, the upper and boundary lines are obtained from regression analysis for data considering a confidence level of 95%. As shown in Fig. 7, the calculated FS from finite element simulation is generally consistent with the predicted FS from Eq. (4.1). In general, the trend of FS shows the consistency between predicted FS and calculated FS. There is also uncertainty appearing in the analysis. Therefore, the boundaries for FS should be determined. In this study, the use of lower and upper boundaries could be implemented. For engineering practice, the use of Eq. (4.1) could be implemented for preliminary investigation of the available FS in the study area.

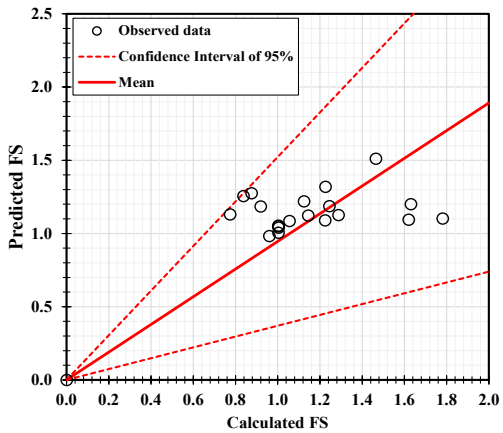

Fig. 7. The comparison between predicted FS and calculated FS at Nakau Segment.

4.3 Slope countermeasure effort

It has been identified that the slope movement could be initially begun at the slope toe. Therefore, the use of a counterweight at the slope toe could be a solution to improve FS for the riverbank slope in Nakau Segment. The slope countermeasure using the combination between gabion and geosynthetic is implemented. Gabion is assumed as a solid rock material. Gabion's model is assumed as a linear elastic and drained material. The unit weight for gabion stone is about 15 kN/m^3 with a coefficient of permeability of 10 m/day. The modulus elasticity of gabion stone is 1.4×10^6 kN/m^2 and Poisson's ratio is assumed as 0.2. Geosynthetic material functions as separation. It is assumed an elastoplastic material with elastic axial stiffness (EA) of about 352 kN/m and a maximum axial tension force of about 21,850 kN/m (adopted from Brinkgreve et al. [40]). Two stages are considered in the analysis. The first one is gravity loadings load and the second one is the reduction of shear strength analysis.

Fig. 8 presents the finite element simulation for slope countermeasure. It can be observed that the implementation of gabion at the slope toe could reduce the potential sliding zone. In addition, its implementation could cut the slip surface. The implementation of gabion in the study area could yield FS varied from 1.525 to 2.049. The average of FS from the implementation of gabion is 1.721, which indicates that the slope reinforcement using the gabion could significantly improve FS. Generally, under the implementation of gabion in the study area, the percentage of gabion varies from 24 to 88%. Maynord [41] and Mase et al. [42] mentioned that the use of gabion as a counterweight at the slope toe could significantly increase slope stability. Yang et al. [43] and Wang et al. [44] also suggested that the use of gabion could effectively reduce the scouring effect at the slope toe. The vegetation protection

on the slope surface also could be implemented to reduce scouring at the slope body [45]. In line with the study area condition, the main cause of slope failure in the riverbank at the Nakau Segment is due to the increase of excess pore pressure at slope mass. Therefore, the implementation of gabion in the Nakau Segment seems to be reasonable.

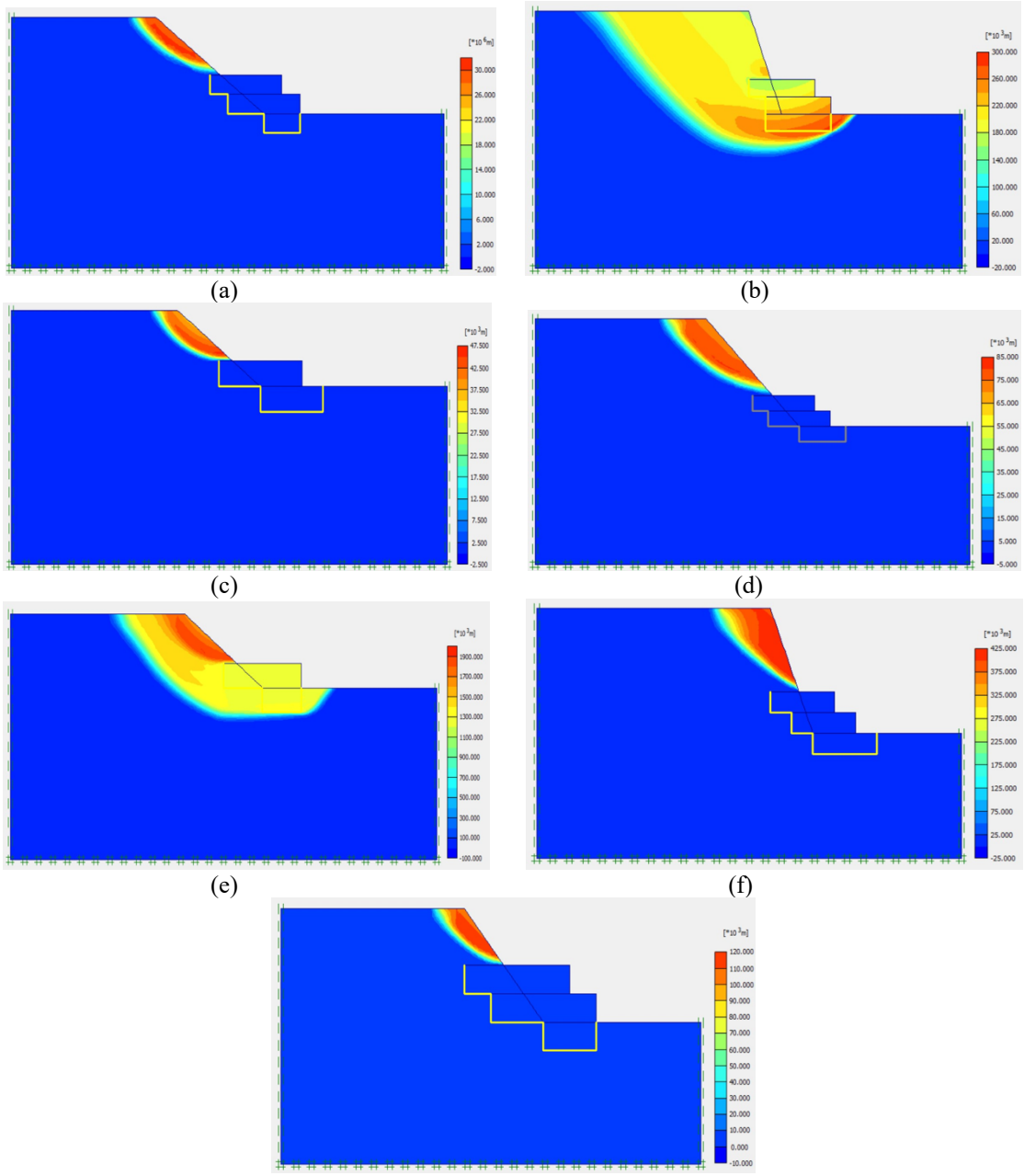

Fig. 8. Failure Mechanism on slopes at Nakau Segment under the implementation of gabion (a) CS-1, (b) CS-4, (c) CS-7, (d) CS-12, (e) CS-13, (f) CS-16, (g) CS-17.

5. Conclusion

Several concluding remarks from this study can be drawn:

1. Slopes along Nakau Segment have been identified as slope failure areas. Based on the investigation of environmental conditions and slope geometry measurements, the steep slope indicates that there is a scouring at the slope toe. The type of failure on this slope is wedging plain failure. Additionally, there is sedimentation indication at a gentle slope. The sedimentation material could behave as dumped material at the slope toe. This could also act as a counterweight at the slope toe. However, the effect of sedimentation and erosion strongly influence the flood flow capacity. Both sedimentation and erosion could play an important role to control slope stability in the study area. The type of failure for a gentle slope is a circular plain failure, whereas for a slope with a steep inclination, the type of failure is a wedge plain failure.

2. The increase of river water level during the flood could decrease shear strength reduction and tend to make a slope to be easier to slide. The soil mass also increases due to saturated conditions. The slope movement initially comes from the movement at the slope toe.

3. The counterweight in the form of gabion could be effectively decreasing sliding plain. Gabion is effective to retain the potentially sliding soil mass. It is also effective to reduce the scouring effect due to the river stream during floods.

4. The proposed equation to predict FS of the riverbank at Nakau Segment could be implemented for engineering practice and adopted by the local government to estimate slope failure potential in the study area.

Acknowledgment

This research was supported by the international collaborative research fund with grant number 1748/UN30.15/PG/2021, from the Institution of Research and Community Services, University of Bengkulu, Indonesia. The authors would like to thank Soil Mechanics Laboratory, University of Bengkulu, for the site investigation and laboratory test performed in this study. This research was partially conducted under the support of the Kurita Water and Environment Foundation (KWEF), Japan in 2018.

References

[1] Misliniyati R, Mase LZ, Syahbana AJ, Soebowo E. Seismic hazard mitigation for Bengkulu Coastal area based on site class analysis. IOP Conf. Ser. Earth Environ. Sci 2018;212(1): 012004.

[2] Mase LZ, Edriani AF, Putra H, Saputra J. Bearing capacity analysis of surficial strip footing at sub-watershed of downstream Muara Bangkahulu River, Indonesia. IOP Conf. Ser. Earth Environ. Sci 2021;871(1): 012051.

[3] Mase LZ, Amri K, Farid M, Rahmat F, Fikri MN, Saputra J, Likitlersuang, S. Effect of Water Level Fluctuation on Riverbank Stability at the Estuary Area of Muaro Kualo Segment, Muara Bangkahulu River in Bengkulu, Indonesia. Eng J 2022;26(3): 1-16.

[4] Mase LZ, Amri K, Frisky M, Anggraini PW, Fikri MN, Agustina S. The effect of flood on slope stability along downstream riverbank of Muara Bangkahulu River, Bengkulu City, Indonesia. In IOP Conf. Ser. Earth Environ. Sci 2021;926(1): 012004.

[5] Mase LZ. Slope stability and erosion-sedimentation analyses along sub-watershed of Muara Bangkahulu River in Bengkulu City, Indonesia. E3S Web. Conf 2020;148: 03002.

[6] Mase LZ. Final Report: A study of climate change and environmental damage impacts of Muara Bangkahulu River Watershed to evaluate the policy in conserving the sub-watershed of Bengkulu Hilir for the local citizen in

Bengkulu City, Indonesia. Kurita Water and Environment Foundation (KWEF); 2019.

[7] Nguyen TS, Likitlersuang S, Ohtsu H, Kitaoka T. Influence of the spatial variability of shear strength parameters on rainfall induced landslides: a case study of sandstone slope in Japan. Arab J Geosci 2017;10(16): 1-12.

[8] Pasculli A, Calista M, Sciarra N. Variability of local stress states resulting from the application of Monte Carlo and finite difference methods to the stability study of a selected slope. Engineering Geology 2018;245: 370-89.

[9] Chheng C, Likitlersuang S. Underground excavation behaviour in Bangkok using three-dimensional finite element method. Comput Geotech 2018;95: 68-81.

[10] Ukritchon B, Keawsawasvong S. Undrained lower bound solutions for end bearing capacity of shallow circular piles in non-homogeneous and anisotropic clays. Int J Numer Anal Methods Geomech 2020;44(5): 596-632.

[11] Mase LZ, Likitlersuang S, Tobita T. Cyclic behaviour and liquefaction resistance of Izumio sands in Osaka, Japan. Mar. Georesources Geotechnol. 2019;37(7): 765-74.

[12] Huynh QT, Lai VQ, Shiau J, Keawsawasvong S, Mase LZ, Tra HT. On the use of both diaphragm and secant pile walls for a basement upgrade project in Vietnam. Innov. Infrastruct. Solut 2022;7(1): 1-10.

[13] Udomchai A, Hoy M, Horpibulsuk S, Chinkulkijniwat A, Arulrajah A. Failure of riverbank protection structure and remedial approach: A case study in Suraburi province, Thailand. Eng. Fail. Anal 2018;91: 243-54.

[14] Duong TT, Do MD. Riverbank stability assessment under river water level changes and hydraulic erosion. Water 2019;11(12): 2598.

[15] Liang C, Jaksa MB, Ostendorf B, Kuo, YL. Influence of river level fluctuations and climate on riverbank stability. Comput Geotech 2015;63: 83-98.

[16] River Territory Office (RTO). Rainfall intensity in Muaro Kualo Area within 2011-2020. Bengkulu, Indonesia: River Territory Office; 2020.

[17] Carter M, Bentley S. Correlations of soil properties. John Wiley & Sons; 2016.

[18] Bowles JE. Foundation design and analysis. New York: McGraw Hill; 1982.

[19] Stark TF, Ruffing DG. Selecting minimum factors of safety for 3D slope stability analyses. In: Huang J, Fenton GA, Zhang L, Griffiths DV, editors. Geo-Risk 2017: Reliability-Based Design and Code Developments, ASCE; 2017, p. 259-66.

[20] Matsui T, San KC. Finite element slope stability analysis by shear strength reduction technique. Soils Found 1999;32(1): 59-70.

[21] Dawson EM, Roth WH, Drescher A. Slope stability analysis by strength reduction. Geotechnique 1999;49(6): 835-40.

[22] Zhang Q, Shuilin WANG, Xiurun GE, Hongying WANG. Modified Mohr-Coulomb strength criterion considering rock mass intrinsic material strength factorization. Min. Sci. Technol 2010;20(5): 701-6.

[23] Dyson AP, Tolooiyan A. Optimisation of strength reduction finite element method codes for slope stability analysis. Innov. Infrastruct. Solut. 2018;3(1): 1-12.

[24] Zhao L, Yang F, Zhang Y, Dan H, Liu W. Effects of shear strength reduction strategies on safety factor of homogeneous slope based on a general

nonlinear failure criterion. Comput. Geotech 2015;63(1): 215-28.

[25] Arvin MR, Zakeri A, Shoorijeh MB. Using finite element strength reduction method for stability analysis of geocell-reinforced slopes. Geotech. Geol. Eng 2019;37(3): 1453-67.

[26] You G, Mandalawi MA, Soliman A, Dowling K, Dahlhaus P. Finite element analysis of rock slope stability using shear strength reduction method. In Frikha W, Varaksin A, Viana da Fonseca A, editors. Soil Testing, Soil Stability and Ground Improvement. GeoMEast 2017. Sustainable Civil Infrastructures. Springer, Cham; 2018. p. 227-35.

[27] Meng Q, Liu Z, Borders BE. Assessment of regression kriging for spatial interpolation–comparisons of seven GIS interpolation methods. Cartogr Geogr Inf Sci 2013;40(1): 28-39.

[28] Gallage C, Abeykoon T, Uchimura T. Instrumented model slopes to investigate the effects of slope inclination on rainfall-induced landslides. Soils Found 2021;61(1): 160-74.

[29] Hampton MA, Lee HJ, Locat J. Submarine landslides. Rev. Geophys 1996;34(1): 33-59.

[30] Seminara G. Meanders. J. Fluid Mech. 2006;554: 271-97.

[31] Zolezzi G, Luchi R, Tubino M. Modeling morphodynamic processes in meandering rivers with spatial width variations. Rev. Geophys 2012;50(RG4005): 1-24.

[32] Shu A, Duan G, Rubinato M, Tian L, Wang M, Wang S. An experimental study on mechanisms for sediment transformation due to riverbank collapse. Water 2019;11(3): 529.

[33] Ikeda S, Parker G, Sawai K. Bend theory of river meanders. Part 1. Linear development. J. Fluid Mech 1981;112: 363-77.

[34] Duong TT, Do DM, Yasuhara K. Assessing the effects of rainfall intensity and hydraulic conductivity on riverbank stability. Water 2019;11(4): 741.

[35] Mizutani H, Nakagawa H, Yoden T, Kawaike K, Zhang H. Numerical modelling of river embankment failure due to overtopping flow considering infiltration effects. J. Hydraul. Res. 2013;51(6): 681-95.

[36] Wang LY, Chen WZ, Tan XY, Tan XJ, Yuan JQ, Liu Q. Evaluation of mountain slope stability considering the impact of geological interfaces using discrete fractures model. J. Mt. Sci 2019;16(9): 2184-202.

[37] Osman AM, Thorne CR. Riverbank stability analysis. I: Theory. J Hydraul Eng 1998;114(2): 134-50.

[38] Thorne CR, Osman AM. Riverbank stability analysis. II: Applications. J Hydraul Eng 1998;114(2): 151-72.

[39] Freeman RE, Ray RO. Landscape ecology practice by small scale river conservation groups. Landsc. Urban Plan 2001;56(3-4): 171-84.

[40] Brinkgreve RBJ, Swolfs WM, Engin, E, Waterman D, Chesaru A, Bonnier, PG, Galavi V. PLAXIS 2D User manual, Plaxis bv; 2010.

[41] Maynord ST. Gabion-mattress channel-protection design. J Hydraul Eng 1995;121(7): 519-22.

[42] Mase LZ, Perdana A, Amri K, Bahri, S. A case study of slope stability improvement in Central Bengkulu Landslide in Indonesia. Transp. Infrastruct. Geotechnol 2021: 1-25.

[43] Yang GL, Liu ZZ, Xu GL, Huang XJ. Protection Technology and Applications of Gabion. In: Chen Y, Zhan L, Tang X, editor. Advances in Environmental Geotechnics. Springer, Berlin, Heidelberg; 2010. p.915-9.

[44] Wang Y, Smith JV, Nazem M. Optimisation of a slope-stabilisation system combining gabion-faced geogrid-reinforced retaining wall with embedded piles. KSCE J. Civ. Eng 2021;25(12): 4535-51.

[45] Matić V. Use of gabions and vegetation in erosion-control works. Arch. Biol. Sci 2009;61(2): 317-22.